Q-SWITCHED AND MODE-LOCKED ERBIUM-DOPED FIBER LASER WITH CO-ZNO SATURABLE ABSORBER

NUSRAT KHAN BINTU

FACULTY OF ENGINEERING

UNIVERSITY OF MALAYA

KUALA LUMPUR

2017

Q-SWITCHED AND MODE-LOCKED ERBIUM-DOPED FIBER LASER WITH Co-ZnO SATURABLE ABSORBER

NUSRATKHAN BINTU

DISSERTATION SUBMITTED IN FULFILMENT OF THE REQUIREMENTS FOR THE DEGREE OF MASTER OF ENGINEERING (TELECOMMUNICATIONS)

FACULTY OF ENGINEERING

UNIVERSITY OF MALAYA

KUALA LUMPUR

2017

UNIVERSITY OF MALAYA

ORIGINAL LITERARY WORK DECLARATION

Name of Candidate: Nusrat Khan Bintu

Matric No: KGE150012

Name of Degree: MASTER OF ENGINEERING (TELECOMMUNICATIONS)

Title of Project Paper/Research Report/Dissertation/Thesis ("this Work"):

Q-SWITCHED AND MODE-LOCKED ERBIUM-DOPED FIBER LASER WITH Co-ZnO (CO-DOPED ZNO) BASED SATURABLE ABSORBER

Field of Study: ENGINEERING SCIENCES (PHOTONICS AND FIBER-OPTIC DEVICES)

i. I do solemnly and sincerely declare that:
ii. I am the sole author/writer of this Work;
iii. This Work is original;
iv. Any use of any work in which copyright exists was done by way of fair dealing and for permitted purposes and any excerpt or extract from, or reference to or reproduction of any copyright work has been disclosed expressly and sufficiently and the title of the Work and its authorship have been acknowledged in this Work;
v. I do not have any actual knowledge nor do I ought reasonably to know that the making of this work constitutes an infringement of any copyright work;
vi. I hereby assign all and every right in the copyright to this Work to the University of Malaya ("UM"), who henceforth shall be owner of the copyright in this Work and that any reproduction or use in any form or by any means whatsoever is prohibited without the written consent of UM having been first had and obtained;
vii. I am fully aware that if in the course of making this Work I have infringed any copyright whether intentionally or otherwise, I may be subject to legal action or any other action as may be determined by UM.

Candidate's Signature Date:

Subscribed and solemnly declared before,

Witness's Signature Date:

Name:

Designation:

ABSTRACT

The aim of this thesis to show beat fiber lasers utilizing a cobalt-doped zinc oxide (Co-ZnO) based saturable absorber. At first, the generation of Q-switching pulces prepare has been effectively proposed and exhibited utilizing a cobalt-doped zinc oxide (Co-ZnO) nanorods as a SA. The proposed Q-switching Erbium-doped fiber laser (EDFL) works at 1559.0 nm utilizing the Co-ZnO SA film. Furthermore, A passive mode-locked EDFL was then shown in light of Co-ZnO nanorods SA using modified cavity. A long spool of SMF was consolidated into an EDFL to measure the depression to work in odd fiber scattering of -4.571 ps2 administration. A steady self-began soliton pilses prepare was created at limit direct energy of 219 mW. The central wavelength and redundancy rate of the laser were 1559.5 nm and 1.007 MHz, respectively. The pulse width and most extreme energy vitality obtained aere 462.8 ns and 5.1 nJ, respectively at a direct energy of 248 mW. The Co-ZnO nanorods film was created by a straightforward preparing procedure, and it has a balance profundity of 6 % and immersing force of 60 MW/cm2.

ABSTRAK

Tujuan tesis ini adalah untuk menunjukkan denyutan gentian laser menggunakan kobalt-doped zink oksida (Co-ZnO) berasaskan penyerap tertepu (SA) Pada mulanya, penjanaan suis-Q telah dicadangkan dan dipamerkan dengan menggunakan nanorod kobalt-doped zink oksida (Co-ZnO) sebagai penyerap tertepu (SA). Suis-Q laser gentian terdop erbium (EDFL) yang dicadangkan beroperasi pada 1559.0 nm dengan mengunnakan filem SA Co-ZnO. Tambahan lagi, mod terkunci pasif telah ditunjukkan dalam cahaya kepada nanorod Co-ZnO. SA menggunakan litar yang telah diubah. SMF yang panjang telah digabungkan ke dalam EDFL untuk mengukur penyebaran gentian ganjil pada 4.571 ps2. Suatu pepejal soliton yang mula digunakan sendiri telah dicipta pada had tenaga terus 219 mW. Pusat panjang gelombang dan kadar redundasi laser adalah 1559.5 nm dan 1.007 MHz. Lebar pulsa dan tenaga daya hidup yang melampau adalah 462.8 ns and 5.1 nJ, asing dengan tenaga terus pada 248 mW. Filem nanorod Co-ZnO telah dihasilkan dengan prosedur penyediaan langsung, dan ia mempunyai keseimbangan sebanyak 6% dan daya tenggelam 60MW/cm2.

ACKNOWLEDGEMENT

In the name of Allah, the most compassionate and the most merciful

Firstly, I would like to express my sincere gratitude to my supervisor prof. DR. Sulaiman Wadi for the continuous support of my MSC final year project, for his patience, and immense knowledge. His guidance helps me in all the research and writhing of this thesis. Special thanks to PHD student researcher Umi

Lastly, I would like to thank my family and my friends for supporting me spiritually throughout writing this thesis and my life in general.

TABLE OF CONTENTS

TABLE OF FIGURE CONTENT

LIST OF TABLE

LIST OF SYMBOLA AND ABBRIVATION

ASE	:	Amplified Spontaneous Emission
CNT	:	Carbon Nanotubes
Co-doped ZnO	:	Cobalt-Doped Zinc Oxide
Co	:	Cobalt
$CoCl_2 \cdot 6H_2O$	:	Cobalt (II) Chloride Hexahydrate
Co_3O_4	:	Cobalt Oxide
CW	:	Continuous-Wave
ECD	:	Electrochemical Deposition
EDF	:	Erbium-Doped Fiber
EDFA	:	Erbium-Doped Fiber Amplifier
EDFL	:	Erbium-Doped Fiber Laser
Er^{3+}	:	Erbium
FESEM	:	Field Emission Scanning Electron Microscopy
FSF	:	Frequency Shifting Feedback
FWHM	:	Full Width Half Maximum
ISO	:	Isolator

MOPA	:	Master Oscillator Power Amplifier
MoS_2	:	Molybdenum Disulfide
OSA	:	Optical Spectrum Analyzer
PLD	:	Pulsed Laser Deposition
PVA	:	Polyvinyl Alcohol
RF	:	Radio Frequency
SA	:	Saturable Absorber
SBS	:	Stimulated Brillouin Scattering
SESAM	:	Semiconductor Saturable Absorber Mirrors
SHB	:	Spatial Hole Burning
SNR	:	Signal to Noise Ratio
TiO_2	:	Titanium Dioxide
Tm^{3+}	:	Thulium
TMDS	:	Transition-Metal Dichalcogenides
WDM	:	Wavelength Division Multiplexing
WS_2	:	Tungsten Disulfide
Yb^{3+}	:	Ytterbium
$Zn(O_2CCH_3)_2 \cdot 2H_2O$	:	Zinc Acetate Dehydrate
Zn	:	Zinc

ZnO	:	Zinc Oxide

CHAPTER 1

Introduction

1.1 Motivation

Optical fiber technology started with the growth of the field of telecommunications. The telecommunication industry has rapidly developed since the first electrical telegraph was patented by Samuel Morse in 1837. Later, the telephone was patented by Alexander Graham Bell in 1878. The developments of laser in 1960s and low loss fibers in 1980s (T & T.Miyashita, 1979)were the breakthrough for telecommunication industry. The low loss fiber was realized using a silica host material. This material (silica) has almost perfect purity in which material absorption and Rayleigh scattering at long wavelengths are at the fundamental limit for optical loss. The minimum loss (about 0.2 dB/km) is found at wavelength of about 1.55 μm. This is the fundamental reason behind that modern telecommunications use wavelength of 1.55 μm. The developments in optical fibers opened the door not only for developments in telecommunications, but also for the birth of fiber lasers.

The research on fiber laser has grown rapidly since Planck discovered that the energy could be emitted or absorbed only in discrete forms which are called quanta. This laser has shown more advantages compared to the other types of lasers such as dye, chemical and solid-state lasers. This is attributed to the ability of this laser to provide better efficiency and also its size is more compact. Light is tightly confined to a small cross-sectional area of an optical fiber and this allows high intensity of light to be generated in the core. High surface area to volume ratio in optical fiber allows excellent heat dissipation, facilitating unprecedented power scaling capacity.

Fiber lasers have been demonstrated in the 1960s by the incorporation of trivalent rare-earth ions such as neodymium (Nd), erbium (Er), and thulium (Tm) into glass host (Wolf, 1964). Soon thereafter Nd has been incorporated into the fiber cores (koester, 1964). Thanks to the high efficiency of the Nd^{+3} ions as a laser, early work was concentrated on Nd^{+3}-doped silica fiber lasers operating at 1.06 μ (koester, 1964). It was until the 1980s that doping of silica fibers with Er+3 ions was achieved (R.J. Mears, 1985). Since that time Erbium-doped fiber lasers (EDFLs) have attracted very much attention. This is because the lasing wavelength at 1.55 μm coincides with the least-loss of silica fibers (as low as 0.15dB/km) and therefore is very suitable for light wave communications.

Pulsed lasers are usually preferred in many applications, including material processing, micromachining, sensing and second harmonic generation. The pulse operation can be realized by two approaches; Q-switching and mode-locking. The basis of Q-switching is to introduce a high loss (or small Q-factor) before lasing in the cavity. This forces the gain medium to build up a relatively high population inversion so that it produces a high gain to match up with the high loss. By switching the Q factor to a higher value, lasing starts rapidly releasing the stored energy in the gain medium. This results in a short pulse incorporating that energy, and thus a high peak power. Q-switching enables the generation of high peak power or high pulse energy with moderate pump power. On the other hand, mode-locking is obtained by inducing a fixed phase relationship among the longitudinal modes in the laser's resonant cavity. The constructive or destructive interference among these modes leads the laser producing a steady train of pulses. These pulses could be of extremely short duration on the order of picoseconds or femtoseconds depending on the design configuration.

In this report we prepared Co-ZnO thin film based saturable absorber (SA) to incorporate into the EDFL cavity to produce Q-switched and mode-locked fiber laser.

1.2 Objectives

The research work aims to demonstrate pulsed fiber lasers using a cobalt-doped zinc oxide (Co-ZnO) based saturable absorber. This research embarks on the following objectives:

- To demonstrate the generation of Q-switching pulses train using the Co-ZnO based SA
- To demonstrate the generation of mode-locking pulses train using the Co-ZnO based SA

1.3 Outline of this report

This report describes an experimental work on Q-switched and mode-locked EDFLs using a Co-ZnO based SA. The content is arranged in 5 chapters, including this introductory chapter and conclusion chapter. Chapter 1 explained the motivation and objectives of this research work. The literature reviews on fiber laser, Q-switching and mode-locking are described in Chapter 2. Chapter 3 describes on the preparation of Co-ZnO SA and the Q-switching results. Chapter 4 describes the mode-locking results using the Co-ZnO based SA. Finally, Chapter 5 concludes the finding of this research and proposes some recommendations for future work.

Chapter 2

Literature Review

2.1 Introduction to optical fiber and lasers

Fiber-optic communication systems, which use optical fibers for data transmission have been commercially deployed since 1980. The system has many advantages such as long-distance transmission, large bandwidth, high security and thus really transformed the telecommunications industries (P.Agarwal, 2003). An optical fiber is a cylindrical dielectric waveguide fabricated from a transparent glass material such as silica glass of high chemical purity. The refractive index of the core is designed to be relatively greater than the cladding index so that light signal can propagate along the fiber axis by the total internal reflection as described in Figure 2 (SALED & TEICH, 1991).

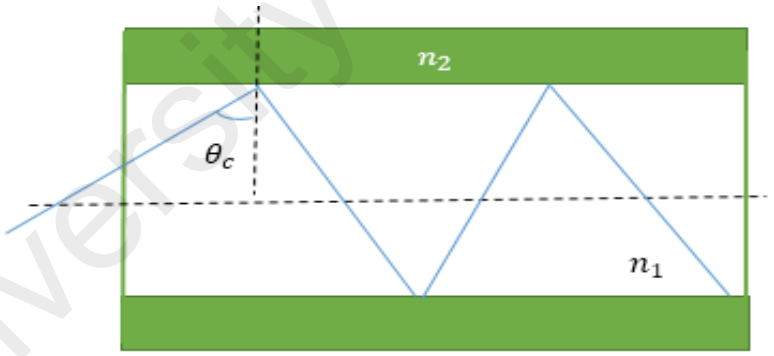

Figure 2.1: The light propagating along the fiber by total internal reflection. θ_c, n_1 and n_2 are critical angle, core refractive index and cladding refractive index, respectively.

Optical fibers are classified into two major types; single mode optical fiber and multimode optical fiber. The core of single mode fiber has a very narrow diameter, which is comparable to the wavelength of the propagating light in practice and thus the light can travel

only one path without a significant reflection of light in the core-cladding interface. The core diameter of multimode fiber is so much larger, and thus allow it to travel in many different paths inside the core. This limit the transmission length of the signal due to inter-symbol interference (ISI). Optical communication systems send data at specific wavelengths that are in the near-infrared portion of the spectrum, directly above the visible band, and thus unnoticeable to the unassisted eye. Generally, optical transmission wavelengths are 0.850 μm, 1.310 μm, and 1.550 μm. Optical communication system consists of an optical source to convert an electrical to an optical signal for sending through the optical cable, a cable containing numerous brunch of optical fibers, optical amplifiers to enhance the power of the optical signal, and an optical receiver to invert the received optical signal into the original transmitted electrical signal (Francis Idachaba, 2014).

Laser is a device that produces light through a process of optical amplification based on the stimulated emission of electromagnetic radiation. It produces light with narrow linewidth, monochromatic, high intensity and excellent directionality. These unique characteristics of laser have made it an important tool in various applications in the areas of communication, military operations, industry, medicine, scientific research and etc. Laser also made significant benefits in surgery, data storage and holography.

A laser device mainly consists of three components; gain medium, resonator and pump as described in Fig. 2.2. The gain medium is where the amplification of light by stimulated emission occur and specifies the operation wavelength. The resonator or laser cavity involves two mirrors placed at the end of the gain medium such that it reflected back and forth the amplified photons at any time passing through the active medium and stimulated another photon so these repeated reflections increases the amplification of the light. One of the two mirrors is partial reflector while the other is total reflector mirror. Pumping process is the process of providing energy needed by the cavity so as to create population inversion

and to get amplification. The energy supplier may be electric source or light source [(palanker, n.d.)].

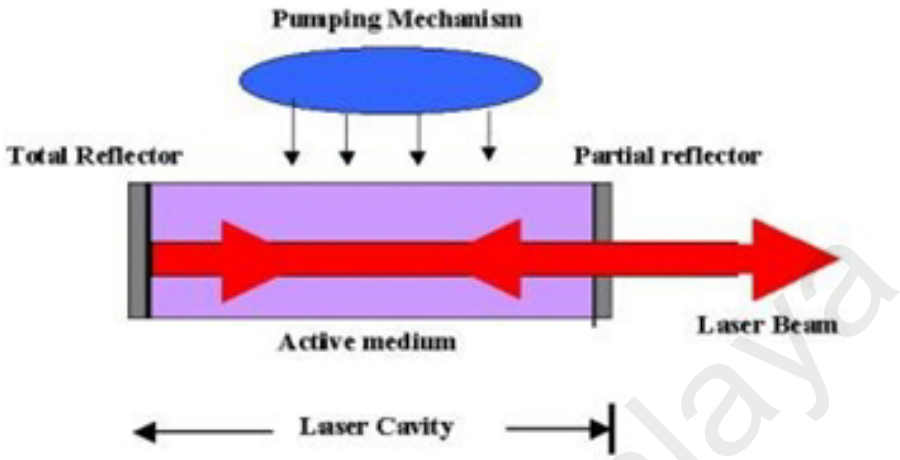

Figure 2.2: Basic structure of laser system which consists of active medium, resonator and pump [(palanker, n.d.)]

2.2 Erbium-doped fiber laser

Fiber lasers use an optical fiber doped with rare earth ions as the gain medium. The creation of rare earth doped fiber has proved to be a versatile material to generate the ultra-short pulses and wide wavelength tuning for various type of applications. Typically, fiber amplifiers and fiber lasers is based on the glass fibers which are doped generally only in the fiber core with laser-active rare earth ions. In the optical fiber, the rare earth elements are commonly used because the glass consists of rare earth ions are optically active. At a shorter wavelength, rare earth ions can absorb light in which it stimulates them into the meta-stable levels as compared to the amplifier or laser wavelength and it allows the light amplification via the stimulated emission. This behavior is very helpful for creating laser, long lifetimes of the metastable states, quantum efficiency also inclined to be high or to amplify the signal at the emission wavelength. The example of the rare earth ions that are using in fiber doped gain medium such as Erbium (Er^{3+}), Praseodymium (Pr^{3+}), Thulium (Tm^{3+}), Neodymium

(Nd^{3+}), Ytterbium (Yb^{3+}), and Holmium (Ho^{3+}). Table 2.1 shows the rare earth ions and its host glasses and also their emission wavelength ranges.

Table 2.1: Common laser-active ions, host glasses and emission wavelength ranges of rare-earth doped fibers.

Ion	Common host glasses	Emission wavelength
Erbium (Er^{3+})	silicate and phosphate glasses	1.5-1.6 µm,2.7 µm, 0.55 µm
Praseodymium (Pr^{3+})	silicate and fluoride glasses	1.3 µm, 0.635 µm, 0.6 µm, 0.52 µm, 0.49 µm
Thulium (Tm^{3+})	silicate and germinate glasses, fluoride glasses	1.7-2.1 µm, 1.45-1.53 µm, 0.48 µm, 0.8 µm
Neodymium (Nd^{3+})	silicate and phosphate glasses	1.03-1.1 µm, 0.9-0.95 µm, 1.32- 1.35 µm
Ytterbium (Yb^{3+})	silicate glass	1.0-1.1 µm
Holmium (Ho^{3+})	silicate glasses, fluoro-zirconate glasses	2.1 µm, 2.9 µm

Since late 1980s the creation of the erbium-doped fiber (EDF) have been using in extensive applications such as an optical source, optical amplifiers and also tunable lasers. Early 1990s, the first effective optical amplifier is the erbium-doped fiber amplifier (EDFA) and it starting well-known in the optical communication industry. Nowadays, it is broadly used in all types of fiber communication systems, mainly wavelength division multiplexed (WDM) systems. The most famous fiber lasers are Erbium-doped fiber lasers (EDFL) have

proved great progress in this few years. EDFL have many benefits which are broad tunable wavelength, smaller size, good beam quality and cheaper cost.

Figure 2.3 illustrates the energy levels of Erbium ions (Er^{3+}) in Erbium doped fiber. The Erbium ions can be excited by a pump power at either 980 nm pump (three level model system) and 1480 nm pump (two level model system). If there is no radiation, the ions is in their ground states $^4I_{15/2.}$ If the light beam is incident on a frequency corresponding system, the ion will be excited to a higher level and pump radiation will happen. If selected at 980 nm, the ions will excite to the level $^4I_{11/2}$. In the level $^4I_{11/2,}$ the lifetime of the ions is approximately 1 μs. The ions easily decomposed to the metastable level $^4I_{13/2}$ with non-radiative transition, such as by releasing heat. This pump can also function straightly at 1480 nm to generate ions straightly to the metastable level $^4I_{13/2}$. In this case, the rapid relaxation would occur to the lowest level in the sub-group level $^4I_{13/2}$ that laser action will take place. Even with a 1480 nm pump is used and it has an optical power conversion efficiency but 980 nm pump have more advantages as compared to 1480 nm which are provides a broad separation between the laser wavelength and pump wavelength, less noise, it cannot stimulate back transition to the ground state. The excited ions make transition to the ground state, either by spontaneous or stimulated emission.

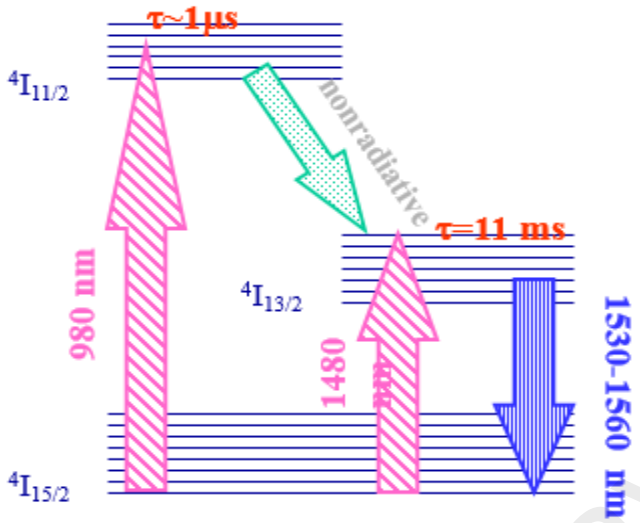

Figure 2.3: *Energy levels of Erbium ions (Er^{3+}) in Erbium doped fiber.*

2.3 Q- switching

Lasers can operate either continuous wave or Q- switch regimes that produces optical power which is limited by a maximum obtainable pump power. When the energy is concentrated in a single pulse of light is called Q-switch and when the energy is a series pulse of light is called continuous wave(CW) (Frungel F. B., 2014). the first Q-switching technique was described in 1961 by Helpworthy, who forecasted that a laser can produce short pulses if suddenly switching cavity losses. And 1962 McClung and Helpworthy was demonstrated experimentally (Mcclung & Hellwarth, 1962). Q-switching is a technique that allows generating extremely short duration and high peak power pulse of light which is much higher than that can be produced by the similar laser working in continuous wave mode.

In principally operation, Q-switching can be achieved by placing a shutter inside laser cavity. If the shutter is closed and we start pumping the gain medium there is no feedback from the mirrors and the laser action is prohibited. There is no stimulated emission and the

population inversion keeps on building up since the pump source raising more atoms from the lower level energy into the higher-level energy. The value of this population inversion is much larger than the threshold population that would be reached in the absence of the shutter for the similar laser operation. If the shutter is now opened spontaneous emission beginning to bounce back and forth through the gain medium. Since the population inversion has been reached a large value, the gain produced by the medium in single round trip exceeds the cavity losses in single round trip so the energy of the laser will grow up rapidly with every round trip. The increasing laser beam utilizes the population inversion, which then reduces quickly and causes reduction the power of the laser beam. Thus, when the shutter is quickly opened a large number of light pulses will be produced. Since this technique relate switching quality factor, high losses indicate low Q-factor while low losses indicate high Q-factor. Therefore, if the shutter is continuing to be closed and rapidly opened, the Q- factor of the cavity is quickly increased from low value to high value and this is called Q-switching. For creating another pulse of light the active medium required to be pumped again while the shutter is remained to be closed and the process repeated again (manna & Saha, 2011).

There are two types of Q-switching active and passive Q-switching. Active Q-switching uses an active control element which are include acoustic optic (manna & Saha, 2011) and electro optic modulator so as to modulate the losses. The most common technique of an active Q-switch is an acousto optic Q-switching that is involved the acousto optic effect. A propagating acoustic wave or standing wave inside the medium changes refractive index of the material periodically because of the periodic straining in the medium and results diffraction of the optical wave. in the presence of standing wave, the medium acts as phase grating. When the acousto optic cell is inserted inside the cavity it diffracted the light beam results to a low Q factor. The value of the Q- factor can be increased by changing the acoustic wave (Ion, 2005)

For the passive Q-switching uses a saturable absorber which inserts inside the resonator.as the intensity of incident light increases the absorption coefficient of the material decreases. This decreasing in the absorption of the material is due to saturation of a transition. Initially the intensity level inside the resonator is small since the saturable absorber does not allow any reflection from the mirror two. if the pumping of the active medium increases, the intensity level inside the resonator increases, which begins to bleach the saturable absorber. This result increasing the feedback reflections that gives growing the intensity of the beam. Therefore, the sored energy in the gain medium is released in form of short pulse of light (manna & Saha, 2011). Unlike active Q-switch the passive Q-switching is cheap and less complexity since it removes the uses of electronic modulators and also can produce extremely high frequency pulse. The production of a well-defined pulse energy and duration which is unaffected by the pumping situations as long as the pump energy is larger than the Q-switching threshold is the main advantage of passive Q switching. However, the passive Q-switching is less efficiencies than for actively Q switching systems since the bleaching of saturable absorber utilizes stored energy. Also, the timing variation of the passive Q switching systems is larger than the active Q switching systems but this is not problem for many ranging applications since the transmitted laser constantly sensed and used timing reference despite of the source properties (Ion, 2005).

Up to now, many different kinds of saturable absorbers including graphene/graphene (jia Xu, 2012, 2014)), carbon nanotube, topological insulators(TIs) (Junsu Lee, 2014)and semiconductor saturable absorber mirrors (SESAM) (Fluck, Braun, Gini, Melchior, & Keller, 1997; Keller et al., 1996) has been demonstrated and utilized. Though in the pulsed laser market the semiconductor saturable absorber mirrors is used commonly since it can be controlled and has flexible design but it has disadvantage such as high fabrication cost, limitation of operation lifetime and bandwidth. Moreover, they are not very simple to

integrate into the fiber laser cavity. 2D nanomaterials (MoS_2 and black prosperous) are the new advanced materials which have better potential because of their wideband respons B. This report demonstrates Q-switched EDFL using cobalt-doped zinc oxide (Co-ZnO) as SA.

2.4 Saturable Absorber

A saturable absorber is an optical component with a certain optical loss, which is reduced at high optical intensities. Saturable absorber can be widely divided into two categories which are real SAs and artificial SAs. Real SAs is materials that exhibit an intrinsic nonlinear decrease in absorption with the increasing light intensity. Artificial SAs is devices that exploit nonlinear effects to duplicate the action of a real saturable absorber by inducing an intensity-dependent transmission. In this part, we only concentrate on real SAs because it has many advantages, such as broadband operation, switching speed and engineer able properties (woodward & Kelleher, 2015). An ideal SA should have high damage threshold but it also makes the cost and time efficient. The primary applications of saturable absorbers are used in Q switching and passive mode locking of lasers, such as the generation of short optical pulses. However, saturable absorbers are also helpful for purposes of nonlinear filtering outside laser resonators, such as for cleaning up pulse shapes and in optical signal processing (D.I.H Mass & A-R bellancourt, 2008).

Fig. 2.4 shows the change of pulse shape when passing through a saturable absorber. As shown in the figure, the low-intensity leading and trailing parts of each pulse are attenuated more strongly than its high-intensity pulse center. This makes the newly formed pulses shorter and shorter over several iterations until a pulse-width of just a few femtoseconds is attained. The width of this pulse then depends on the gain bandwidth of the gain material and on the response time of the saturable absorber. The more frequencies that the gain material produces in a laser, such as the more modes generated inside the laser cavity,

the narrower a pulse. Similarly, as a general trend, the faster a saturable absorber can respond to light, the shorter the pulse (Jonah Maxwell Miller, 2011).

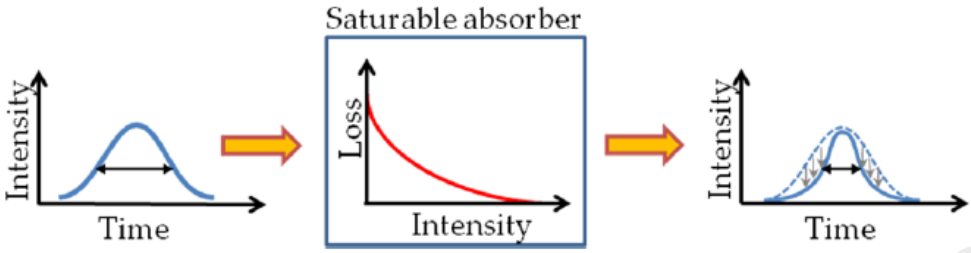

Fig. 2.4: *When passing through a saturable absorber, the low-intensity "wings" of a pulse experience higher loss than the intense pulse center. This causes the duration of the pulse to shrink.*

2.5 Mode-locked Fiber Laser using Saturable Absorber (SA)

The simple meaning of mode-locking techniques is the phase-locking of many longitudinal cavity modes. It was created to induce self-amplitude-modulation (SAM) effect on the propagation of pulse. This process can generate high pulse repetition rate with narrow pulse width and ultra-short pulse from fiber laser into picoseconds and femtosecond duration. The mode-locked techniques are almost similar to Q-switched technique except difference in the optical phase of pulse where mode-locked laser has discreet coherent phase while Q-switched does not have. In this scope of research, two techniques to generate mode-locked pulse laser is active and passive techniques. Although the first stable passive mode-locked pulse laser using SA was proposed in 1990's using SESA (Keller & Chiu, 1992), the unstable mode-locked or Q-switched mode-locked was been found before that.

An active mode-locking happen when optical modulation device was inserted into the cavity to make the round-trip phase change and reduce modulation losses. Acoustic-optic and electro-optic modulator is the popular optical modulation devices used in the cavity to

generate active mode-locking (Mikael Malmström, 2016). A passive mode-locking pulse is produced using SA or self-synchronization using polarization controller (K. Tampura, 1993). The role of SA in the passive technique is to absorb the light enter linearly into the cavity until it reaches at certain intensity. When it achieved at certain level of intensity, the SA saturates becomes clear and it support of pulse production over CW. There are so many different between active and passive mode-locked which are passive mode-locked is more simplicity in fabrication, able to generate pulse without external control devices, and cheaper compare to active. Mode-locked pulse is form when several difference phases are locked together as shown in Figure 2.5.

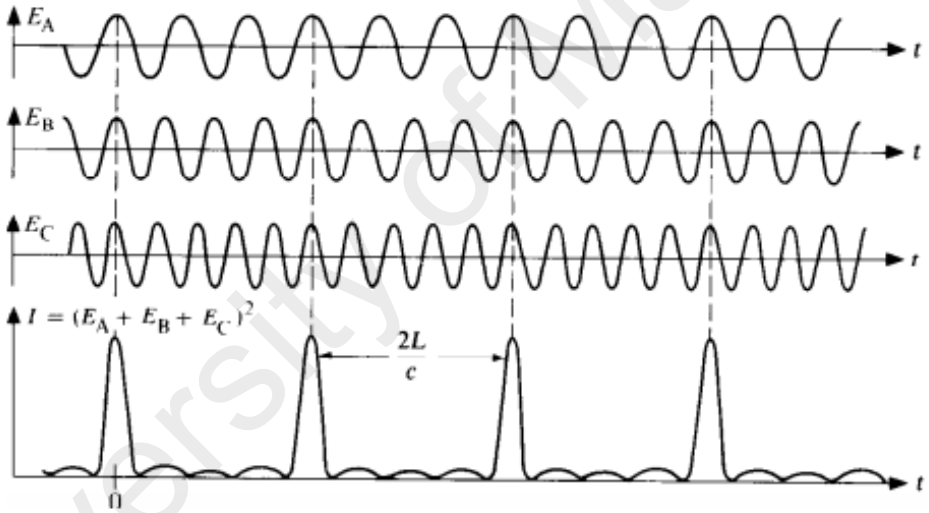

Figure 2.5: *Different phase locking*

2.6 Parameter of pulsed laser

Several important parameters are used to evaluates and characterize the performances of pulse such as pulse width, pulse energy, peak power, and repetition rate. Figure 2.6 shows the important pulse characteristic.

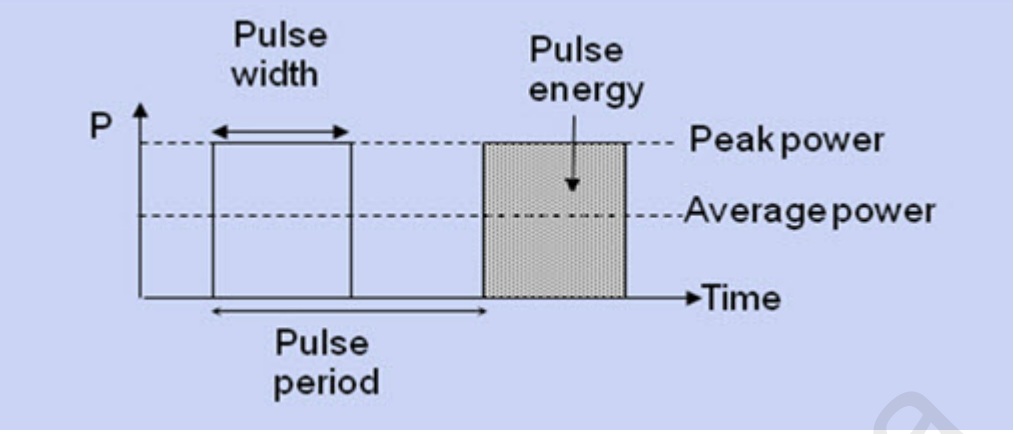

Figure 2.6: Pulse characteristics (America, 2016)

2.6.1 Pulse Width (Δt)

The pulse width is defined as the temporal length of laser pulse that is the time during which the laser actually produce energy or also known as full width at half-maximum (FWHM) of the optical power versus time. The pulse width controls the heat into the part, weld width and thermal heat cycle. For Q-switching laser, the pulse width is generating with duration in between nanoseconds, while for mode-locked laser, the pulse width is generating with duration in between picoseconds or femtoseconds (R. Paschotta, 1997).

2.6.2 Pulse Energy ($\boldsymbol{P_E}$)

Pulse energy (P_E) is defined as the total optical energy content of a pulse, for example, the integration of optical power over time. For Q-switching laser, the pulse energy is normally in range from micro joules to milli joules while for mode-locked, the pulse energy much lower in range pico joules and nano joules. Typically, the pulse energy is calculated by the average power divided to the pulse repetition rate.

$$P_E = \frac{P_o}{R_r}$$

where P_o is average output power and R_r is a repetition rate

2.6.3 Peak Power (P_p)

Peak power (P_p) is defined as the maximum level of optical power in a pulse. The peak power can be calculated mathematically from pulse energy and pulse width by using following formula,

$$P_p = f_s \frac{P_E}{\Delta t}$$

where f_s is the numerical factor. The numerical factor depends on the shape of the pulse. For example, Gaussian-shaped pulses using the factor of ~ 0.94 while f_s equals to 0.88 is used for $sech^2$-shaped pulse. Peak power can be calculated once the pulse shape is known.

2.6.4 Repetition Rate ($\boldsymbol{R_r}$)

Repetition rate (R_r) is defined as the number of pulses emitted per second or the reverse pulse temporal distance. The repetition rate is inversely proportional to the pulse width. For Q-switching laser, the repetition rate is changed by changing the pump power, while for mode-locked laser, the repetition rate is constant on the length of the laser cavity.

2.6.5 Slope efficiency / Laser efficiency

Slope efficiency or laser efficiency is one of the important parameter to evaluate the performance of a laser. It can be find by plotting the graph of output power versus the pump power. To achieve an optimum efficiency of laser output power for a given pump power is normally needs a compromise between the higher slope efficiency and lower threshold pump power. Laser efficiency is a pump power is converted into laser output power.

$$\Pi = \frac{P_{out}}{P_{pump}}$$

where P_{out} is the output power of the laser and P_{pump} is the pump power of the laser.

Chapter 3

Cobalt-doped Zinc Oxide Nanorods as saturable absorber in passively Q-switched fiber laser

3.1 Introduction

Q-switched fiber laser is a kind of pulse laser which could generates high energy pulses up to several milli-joules (I.Hartl, 2013). It has gained significant applications in many fields including medicine, sensing, metrology, optical communication and others (Nishizawa, 2014) (R. Holzawarth, 2000). Q-switching operation can be realized by 2 methods: active Q-switching and passive Q-switching. The former usually utilizes an acousto-optic or electro-optic modulator to modulate the loss of laser resonator (J.-H Lin, 2007), while the latter works with a saturable absorber (SA), which could be semiconductor saturable absorber mirror (SESAM) (J. Liu, 2012), carbon nanotubes (CNTs) [6], graphene (M. A. Ismail, 2012). Some new SAs such as topological insulator (Z. Sun, 2010), black phosphorus (J. Sotor, 2014) and transition metal dichalcogenides (TMD) can also be used in fiber lasers. For instance, Z. Luo et al. used a broadband few-layer MoS_2 SA to Q-switch 1, 1.5 and 2 μs fiber laser (E. Ismail, 2016). Nevertheless, there are still many research efforts

to seek for new high-performance and low cost SAs with ideal characteristics of broadband operation, large modulation depth and high damage threshold.

Recently, transition metal oxides such as zinc oxide (ZnO) have gained a tremendous research interest since they have optical properties complementary to graphene. For instance, ZnO has outstanding properties such as its similar band gap to titanium dioxide, low cost, chemical stability and non-toxicity (L. Li, 2016) (M. H. M. Ahmed, 2016). ZnO is also an important semiconductor material with expansive band gap of 3.3 eV and abundant exciton binding energy of 60 meV (S. G Kumar, 2017) which extensively been used in the optoelectronic instruments such as photodetectors for UV spectral range and laser diodes (O. A. Yildrium, 2016). Various deposition methods are used to fabricate ZnO films including electrochemical deposition (ECD) technique, thermal oxidation, magnetron sputtering, pulsed laser deposition (PLD).

In an earlier work, Ahmad et al. reported passively Q-switched fiber laser using ZnO thin film as SA (S. C, 2016). In this letter, we demonstrate Q-switched Erbium-doped fiber laser (EDFL) using cobalt-doped ZnO (Co-ZnO) nanorods, which is embedded into a polyvinyl alcohol (PVA) film as a passive Q-switcher. MoS2 and BP based SA as a passive Q-switcher. SA with thin-film form has advantages in the mass preparation, uniform quality and flexibility of usage.

3.2 SA Preparation

In our experiment, Co-ZnO nanorods are embedded in PVA to fabricate Co-ZnO-PVA SA film. The Co-ZnO nanorods solution is prepared by adding 0.025 M of Zinc Acetate Dihydrate [$Zn(O_2CCH_3)_2 \cdot 2H_2O$, Friendemann Schmidt Chemical] and 1% of Cobalt (II) Chloride Hexahydrate [$CoCl_2 \cdot 6H_2O$, Sigma Aldrich] dissolved in 100 ml of Isopropanol. The solution is slowly stirred on the hot plate for 2 hours at 60^{o}C. Fig. 3.1 shows a field emission

scanning electron microscopy (FESEM) image of the Co-ZnO solution. It shows the nanorods size of about 300 nm x 6 μm.

The PVA solution was prepared by dissolving PVA powder [10000 MW, Sigma Aldrich] into 80 ml of DI water. The solution was stirred at 145^{o}C until all the powder completely dissolved. To fabricate the thin film, Co-ZnO solution was mixed with PVA solution, then the mixture was slowly stirred for about 2 hours. Then, the mixture solution was poured into the petri dish and left dry in ambient for 3 days. After dry, the thin film was slowly peeled out. It is then cut into a small piece to attach into an FC/PC fiber ferrule as shown in Fig. 3.2. The ferrule was then matched with another fresh ferrule via a connector after depositing index matching gel onto the fiber end to construct an all-fiber SA device.

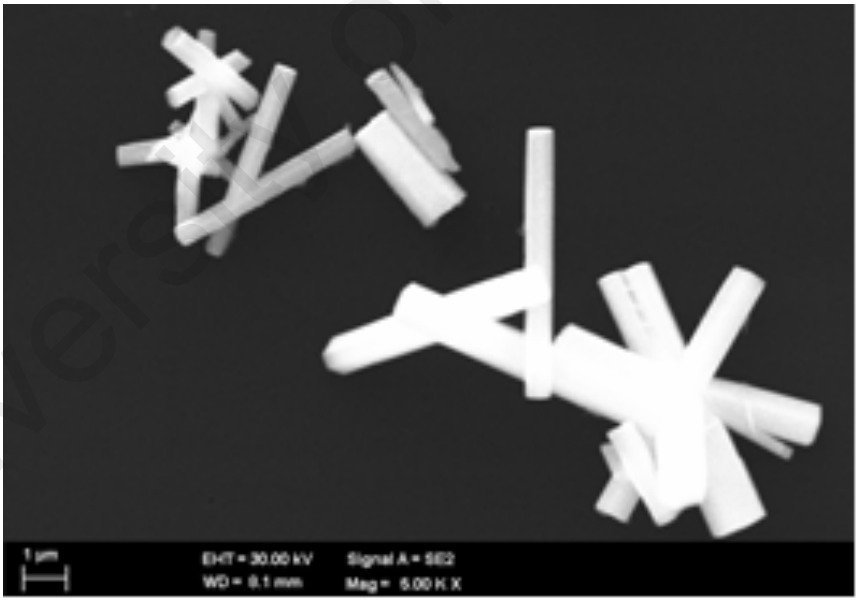

Fig. 3.1: FESEM image of the prepared Co-ZnO nanorods solution

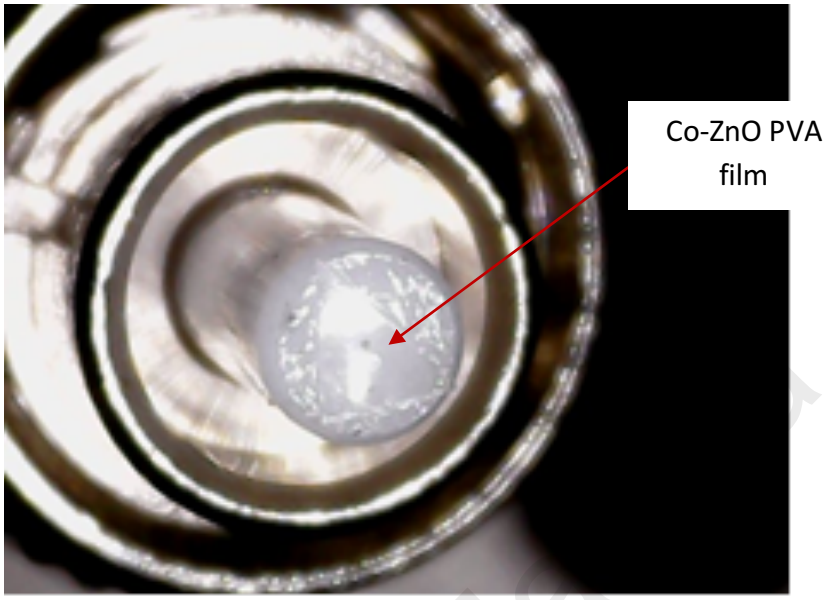

Fig. 3.2: Co-ZnO PVA film onto the end surface of the ferrule

3.3 Q-switched laser configuration

The fabricated SA device was integrated into an EDFL cavity for Q-switching generation as shown in Fig. 3.3. The cavity uses a 2.8-m-long erbium-doped fiber (EDF), which was pumped by a 980-nm laser diode (LD) via a 980/1550 nm wavelength division multiplexer (WDM). The EDF used has a numerical aperture (NA) of 0.16 and erbium ion absorption of 23 dB/m at 980 nm with core and cladding diameters of 4 µm and 125 µm, respectively. To ensure unidirectional propagation of the oscillating laser in the ring laser cavity, a polarization-independent isolator was used. The laser signal was coupled out using 80:20 output coupler while keeping 80% of the light oscillating in the ring cavity for both spectral and temporal diagnostics. The output laser was tapped from a 20% port of the coupler. The spectral characteristic was measured using an optical spectrum analyzer (OSA) with a spectral resolution of 0.02 nm while the temporal characteristics were measured using

a 500 MHz oscilloscope and a 7.8 GHz radio-frequency (RF) spectrum analyzer via a 1.2 GHz photodetector. The total cavity length of the ring laser is about 6 m.

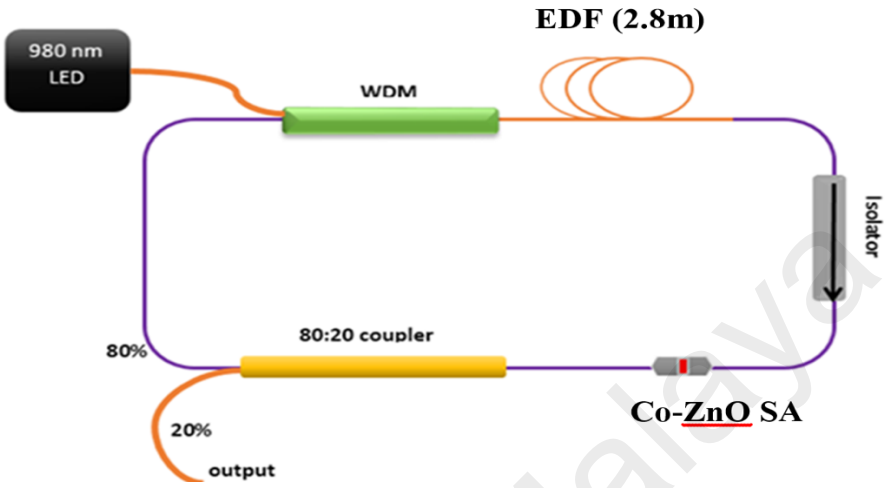

Fig. 3.3: Configuration of the Co-ZnO PVA film based Q-switched EDFL

3.4 Q-switching performance

In this experiment, the pump power was slowly increased until we obtained a stable Q-switched pulse train when the pump power exceeds lasing threshold. Stable, robust and self-starting Q-switching operation is obtained at pump power threshold of 30.5 mW. There is no lasing below the threshold pump power. Such a low threshold power for Q-switching operation results from the small intra-cavity loss performed by the Co-ZnO PVA SA. The Q-switching operation was maintained up to pump power of 109.4 mW. The spectrum of the Q-switched pulse train at pump power of 109.4 mW is shown in Fig. 3.4. It operates at1559.0 nm with a slight spectral broadening due to the self-phase modulation effect in the ring cavity.

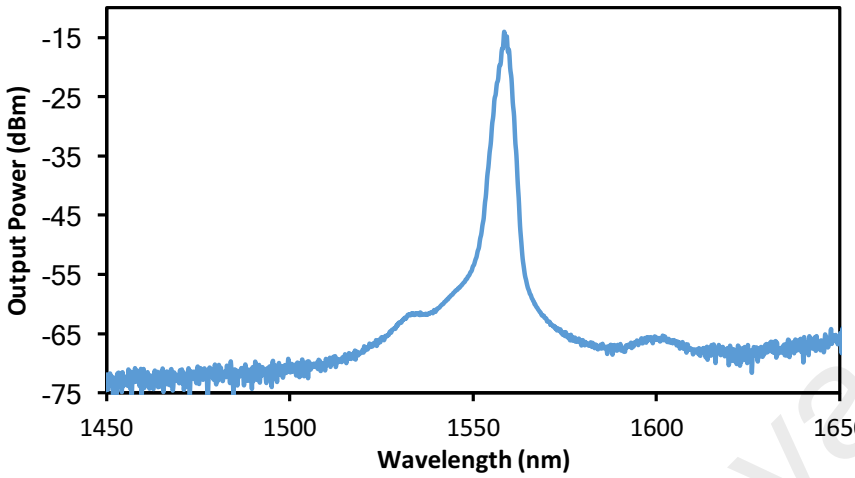

Fig. 3.4: Output spectrum of the Q-switched laser at pump power of 109.4 mW

A stable pulse train with an increasing repetition rate was observed within the pump power from 30.5 to 109.4 mW, which is a typical characteristic for the Q-switched laser (H. Ahmad, 2016). Figure 3.5 shows the typical oscilloscope trace of the Q-switched pulse train at the pump power of 109.4 mW. It shows the peak-to-peak duration of 12.6 µs, which is equal to the repetition rate of 79.4 kHz. It is also observed that the Q-switched pulse output is stable and no amplitude modulations in the pulse train can be observed, which indicates that there is no self-mode locking effect during the Q-switching operation. A single Q-switching pulses is observed to has an almost symmetric shape with a pulse width of approximately 4.62 µs. To verify that the passive Q-switching was attributed to the Co-ZnO PVA SA, the film was removed from the ring cavity. In this case, no Q-switched pulses were observed on the oscilloscope even when the pump power was adjusted over a wide range. This finding confirms that the Co-ZnO PVA SA was responsible for the passively Q-switched operation of the laser.

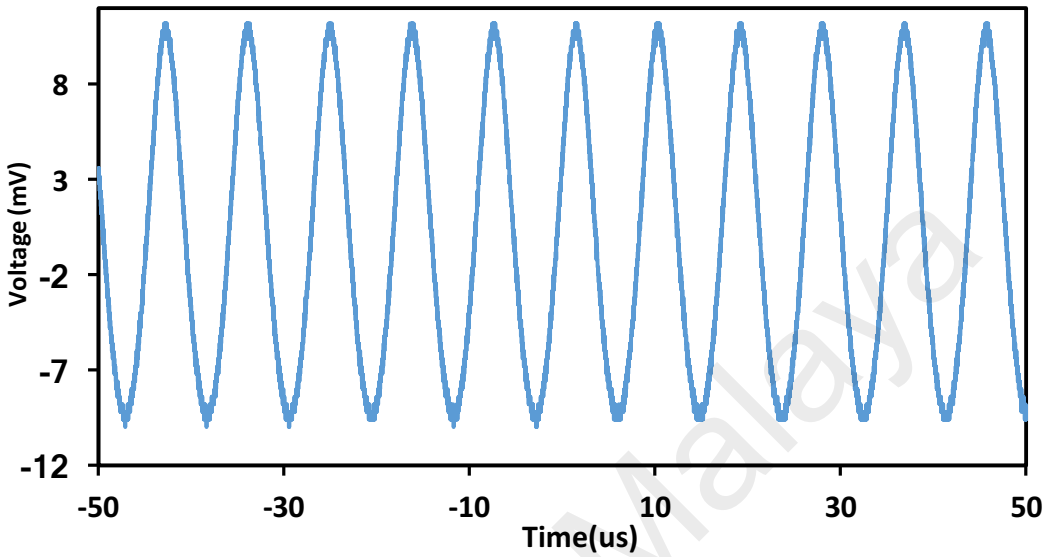

Fig. 3.5: Typical Q-switching pulses at pump power of 109.4 mW

As for the stability of Q-switching operation, we measure the signal to noise ratio of electrical signal transformed by photodiode and analyze electrical spectrum with the help of electrical spectrum analyser (ESA). Fig. 3.6 shows the electrical spectrum at pump power of 109.4 mW. As illustrated in the figure, the fundamental repetition rate of the laser is obtained at 79.4 kHz with a signal-to-noise ratio of 40 dB. This indicates that the Q-switching operation is stable. Agree to Fourier transform, the peak of fundamental repetition rate gradually decrease until the 7th harmonic. Throughout the experiment, we can confirm that no mode-beating frequency presence.

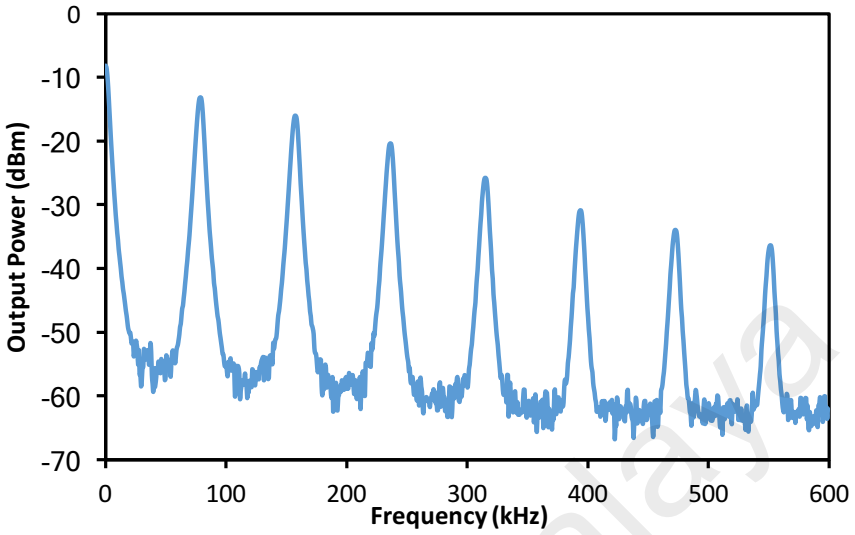

Fig. 3.6: Electrical spectrum at pump power of 109.4 mW

The pulse repetition rate and pulse width of the MoS2 based Q-switched EDFL are investigated as functions of pump power. The results are plotted in Fig. 3.7, which indicates that the repetition rate of the Q-switching pulses can be increased from 56.1 kHz to 79.4 kHz as the power of the pump is varied from 30.5 mW to 109.4 mW. Concurrently, the pulse width decreased from 7.30 µs to 4.62 µs. The pulse width could be decreased further by either shortening the laser cavity length. In addition, the average output power and the corresponding single-pulse energy of the laser are also investigated at various pump powers. The results are plotted in Fig. 3.8. It shows that both average output power and pulse energy increase with the increase of input pump power. The maximum average output power of the Q-switched laser is 11.31 mW while the slope efficiency is calculated to be around 7.79%. The slope efficiency is reasonably high due to the relatively low cavity loss. The maximum pulse energy of 142 nJ is obtained at the maximum pump power of 109.4 mW. This Q-

switching performance could be further improved by optimizing the cavity design and the SA parameters such as modulation depth and insertion loss.

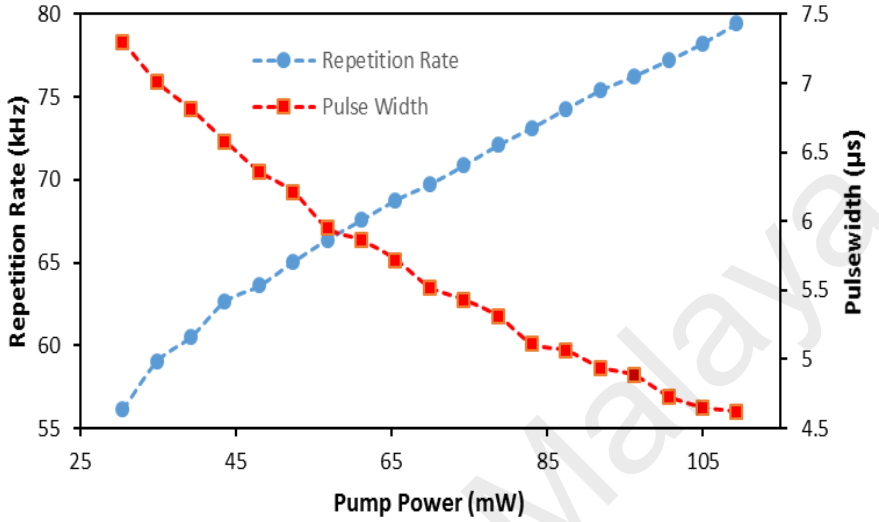

Fig.3.7: the pulse repetition rate and pulse width against pump power

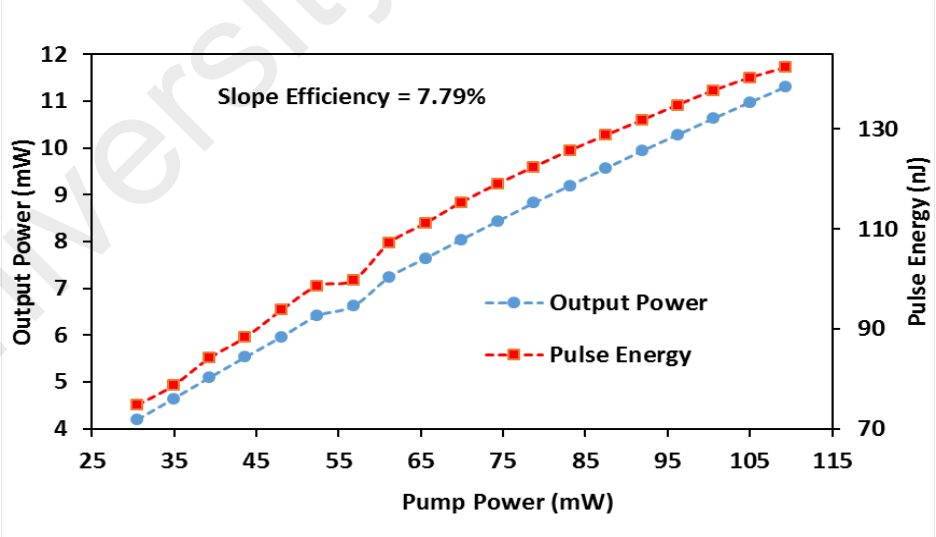

Fig. 3.8: The average output power and the corresponding single-pulse energy against pump power

Chapter 4

Mode-locked Erbium doped fiber laser employing Co-ZnO PVA film as saturable absorber

4.1 Introduction

Mode locking of lasers allows the creation of ultra-short pulses that can be used in a many different application both practical (such as laser cutting and welding) and also for fundamental research. Such lasers systems are the essential component of optical frequency combs which allow measurements of frequency (and thus time) with unparalleled accuracy. Thus, new ways to mode-lock lasers are always important and this work demonstrates the use of novel materials for this application. Mode-locked fiber lasers are powerful sources of ultra-short pulses. They have the advantages over solid-state pulse lasers in the system robustness, beam quality, pumping efficiency, power scalability and easy operation. Due to these advantages, the laser has gained tremendous interest in recent years for various applications such as optical communication, micromachining, metrology and military systems, spectroscopy and laser surgery (Wang, 2004) (Yakuphanoglu, 2010). Mode-locking operation can be realized by either active or passive techniques. The active technique usually employs an acousto-optic or electro-optic modulator to lock the modes in the cavity (A. S. Risbud, 2003), while the passive technique uses a saturable absorber (SA) as a mode-locker. The SA could be semiconductor saturable absorber mirror (SESAM) (M. H. Huang, 2001), carbon nanotubes (CNTs) and graphene (Funda Aksoy Akgul, 2016). Recently, topological insulator (M. Venkatesan, 2004), black phosphorus (R. WisnieWski Jakuda, 2008) and transition metal dichalcogenides (TMD) were also demonstrated for generating mode-locking pulses in various fiber laser cavities. Nevertheless, there are still many research

efforts to seek for new high-performance and low cost SAs with ideal characteristics of broadband operation, large modulation depth and high damage threshold.

In the previous chapter, a passively Q-switched fiber laser was demonstrated using cobalt doped zinc oxide (Co-ZnO) thin film as SA. In this chapter, a mode-locked Erbium-doped fiber laser (EDFL) is demonstrated using the similar SA. An additional spool of single-mode fiber is added into the EDFL cavity to adjust the dispersion and nonlinearity characteristics of the cavity and thus enable mode-locking pulses train generation.

4.2 Modulation depth measurement and laser configuration

In our experiment, Co-ZnO nanorods are embedded in PVA to fabricate Co-ZnO-PVA SA film. Fig. 4.1 shows the FESEM image of the SA thin film, where the darker color indicates the Co-ZnO inside the PVA composite. The film was cut into a small piece to attach into an FC/PC fiber ferrule, which was then matched with another fresh ferrule via a connector to construct an all–fiber SA device. The insertion loss of the SA is measured to be around 1.5 dB at 1550 nm.

A balance twin detector measurement was carried out in order to investigate the nonlinear optical absorption property of Co-ZnO thin film, and thus determines the modulation depth for the SA. An output source of mode-locked pulses with (repetition rate of 1.0 MHz, pulse width 413.0 ns and central wavelength of 1562 nm) was amplified by a low dispersive optical amplifier and split into two ports by a 3dB coupler. One port was directly connected to a photo-detector and another port was used to launch light into the SA device. The output power from both detectors were recorded as the value of attenuation is gradually decreased. From the result, the nonlinear optical absorption was calculated and fitted using the saturation model;

$$\alpha(I) = \frac{\alpha_s}{1+\frac{I}{I_s}} + \alpha_{ns} \quad (4.1)$$

where α(I) is the absorption rate, α_s is the saturable absorption, α_{ns} is the non-saturable absorption, I is the input intensity and I_s is the saturation intensity. As shown in Fig. 4.2, the modulation depth and saturation intensity of Co-ZnO-SA were determined to be 6% and 60 MW cm^{-2} respectively. The non-saturable absorption was 4%.

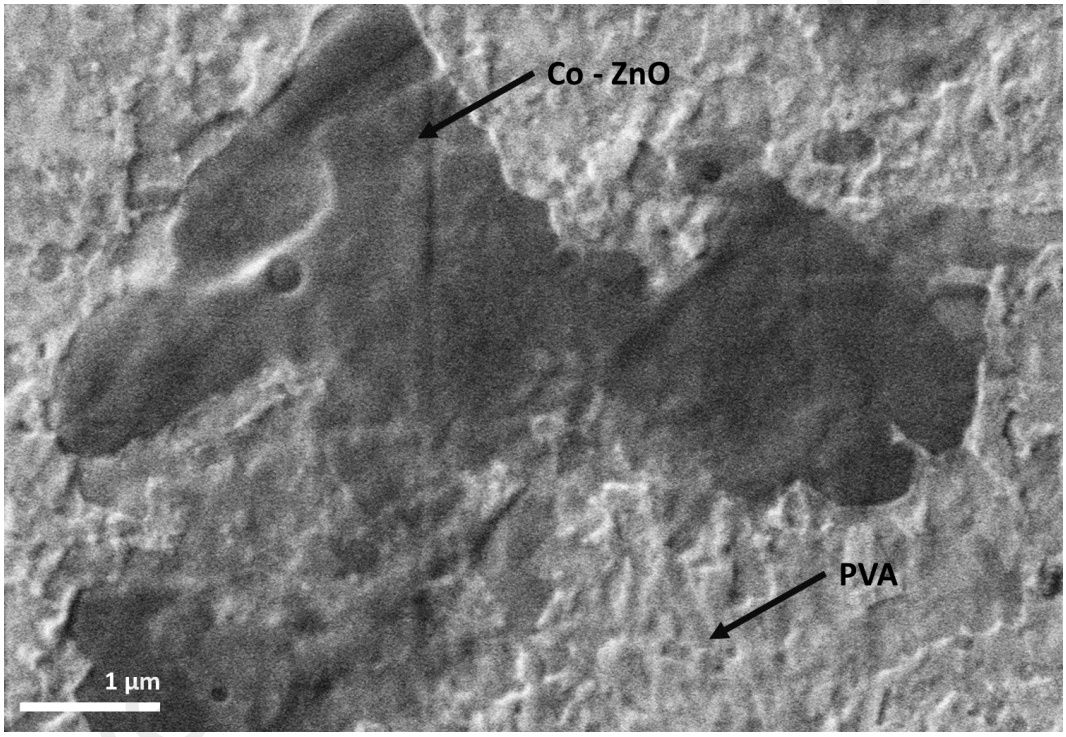

Fig. 4.1. FESEM image of the Co-ZnO PVA film

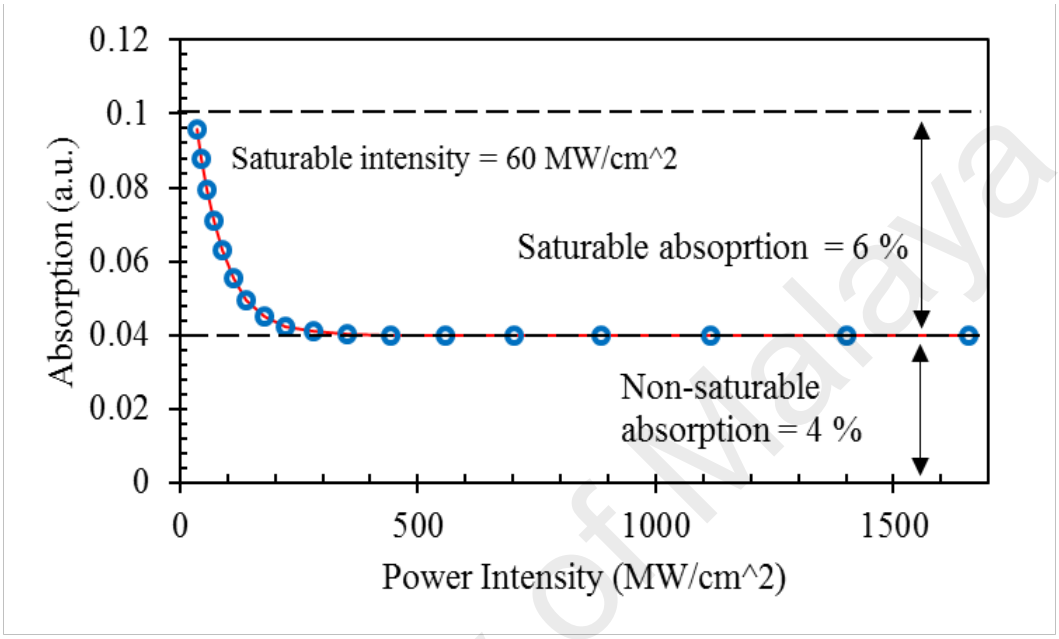

fig.4.2; the absorption profile of the Co-Zno based SA

The fabricated SA device was integrated into an EDFL cavity for generating mode-locking pulses. Fig. 4.3 shows the configuration of the ring laser, which the cavity employs a 2.4-m-long erbium-doped fiber (EDF) as a gain medium. The EDF used has a numerical aperture (NA) of 0.16 and erbium ion absorption of 23 dB/m at 980 nm with core and cladding diameters of 4 µm and 125 µm, respectively. It was pumped by a 980-nm laser diode (LD) via a 980/1550 nm wavelength division multiplexer (WDM). A polarization independent isolator is incorporated in the laser cavity to ensure unidirectional propagation of the laser light. The output of the laser is tapped out of the cavity through 10% port of the output coupler while keeping 90% of the light to oscillate in the laser cavity. The optical

spectrum analyser (OSA) is used to analyse the spectral characteristic of the mode-locked EDFL with a spectral resolution of 0.07 nm whereas the oscilloscope is used to observe the output pulse train of the mode-locked operation via a 460 kHz bandwidth photo-detector (Thor lab, PDA50B-EC). Additional 193 m long standard SMF-28 was added into the cavity to tailor the total group velocity dispersion (GVD) as well as to increase the nonlinearity effect so that mode-locked output pulse can be realized. The mode-locked EDFL has total cavity length of 200.4 m which consists of 2.4 m long EDF and 198 m long SMF, with group velocity dispersion (GVD) of -21.0 ps2/km, and -21.7 ps2/km, respectively. The cavity operates in anomalous fiber dispersion of -4.571 ps2, and thus traditional soliton tends to be formed in the fiber laser.

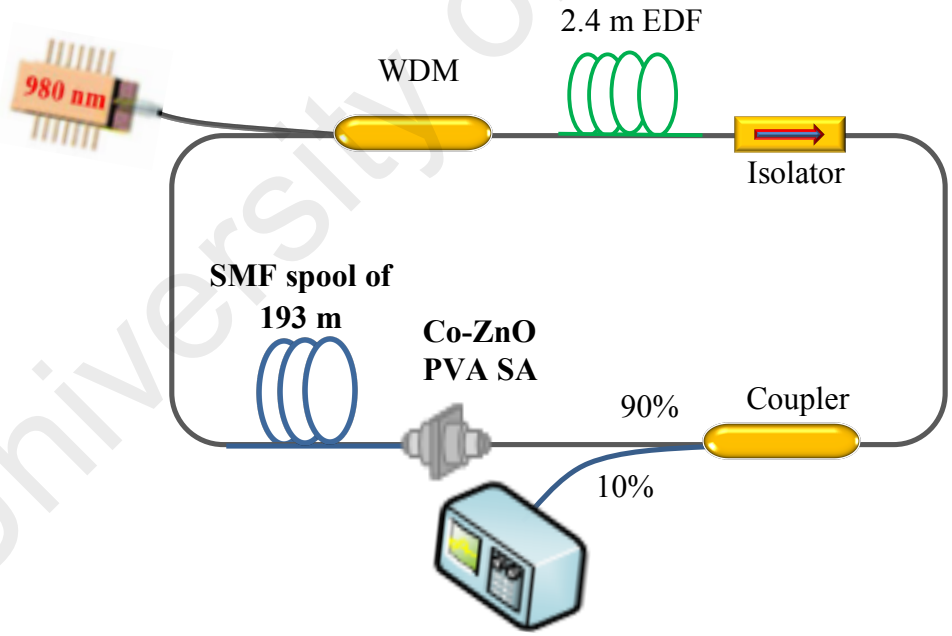

Fig. 4.3: Configuration of the mode-locked EDFL with Co-ZnO PVA film based SA

4.3 Performance of the mode-locked EDFL

With the addition of a long spool of SMF, the balance between the GVD and nonlinearity effect inside the ring cavity allows the generation of a stable mode-locking pulse. During our experiments, continuous-wave (CW) lasing was observed at around 25 mW pump power and the mode-locking laser operation was self-started when the pump power was increased to 219 mW. The output vs. pump power curve is plotted in Fig. 4.4. We achieved a maximum output power of 5.13 mW under 248 mW pump power that was maximally available in the lab, and no output saturation behavior was observed at the top power level. For further confirmation, no mode-locking pulses were observed when Co-ZnO PVA film was removed during testing, indicating the mode-locked laser operation was indeed introduced by the fabricated Co-ZnO SA instead of the nonlinear polarization rotation. Fig. 4.5 illustrates the optical spectrum of the mode-locked EDFL at the pump power of 244 mW. The spectrum is centered at 1559.5 nm with a 3 dB bandwidth of 0.4 nm. Kelly sidebands are also observed on both sides in the spectrum, indicating soliton mode-locked pulse in the anomalous dispersion regime. Inter-correlation between dispersion and nonlinearity in the ring cavity produces a good generation of soliton pulses. The stable self-starting mode-locked could be initiated without any adjustment to the polarization state of the cavity. This indicates that the mode-locked pulses are polarization independent, no polarization controller is required to control the polarization.

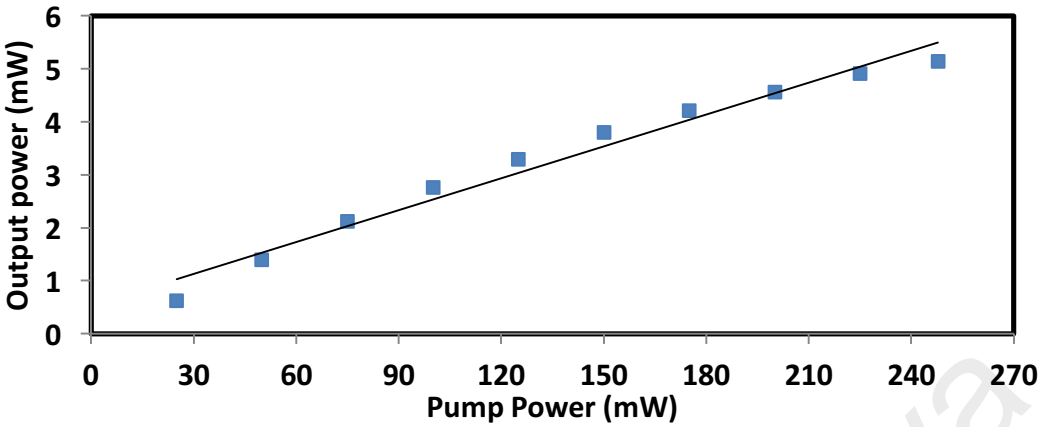

Fig. 4.4: Output power of the EDFL against the pump power.

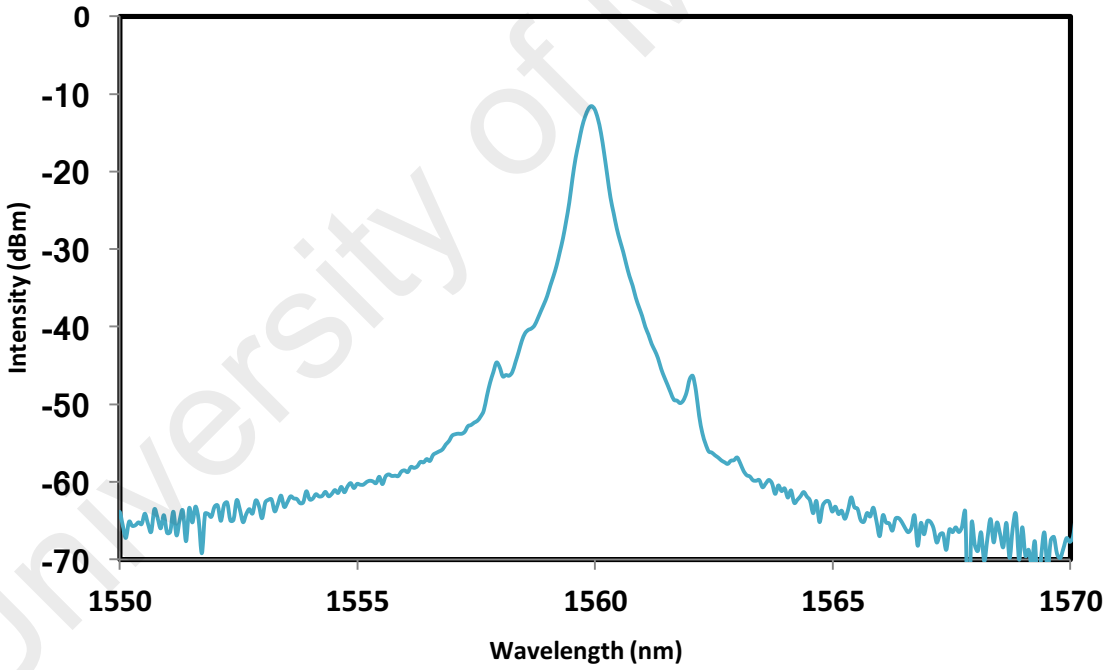

Fig. 4.5: Output spectrum of the mode-locked EDFL at pump power of 244 mW.

Fig. 4.6(a) shows the oscilloscope trace at 244 mW pump power, which indicates a stable mode-locked pulse. The pulse train is uniform and no distinct in amplitude is observed for each envelope spectrum. The peak to peak period of the pulse train is measured to be 992.8 ns, which correspond to the repetition rate of 1.007 MHz. The obtained repetition rate matches with the cavity length of about 200.4 m. Fig. 4.6(b) shows a single envelop of the mode-locked pulse with a pulse duration of about 462.8 ns and the time-bandwidth product is calculated to be 21679.487, which indicates that the optical pulse is heavily chirped. The large frequency chirp obtained verifies that the generated pulse is a dissipative soliton, and its formation is a natural consequence of the mutual balance between the gain, loss, dispersion and nonlinearity characteristics inside the cavity.

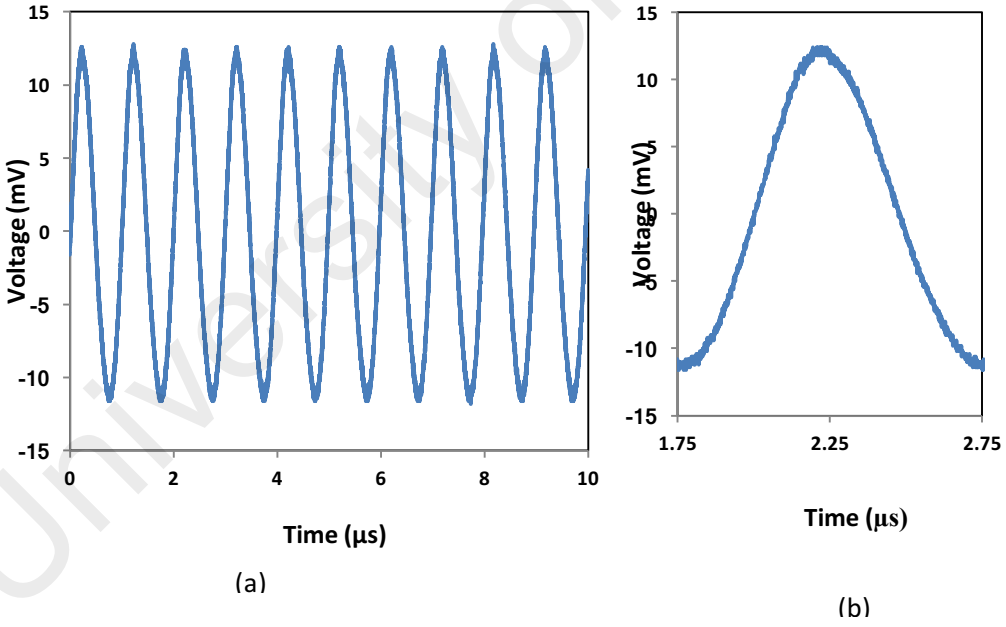

Fig. 4.6: Temporal characteristics of the laser (a) Typical pulses train (b) single pulse envelop

It is clearly shown that the peak power increases from 7.7 to 9.7 mW as the pump power is varied from 219 to 248 mW. On the other hand, the pulse energy also almost linearly increases with the pump power from 4.74 to 5.1 nJ. We observed a constant pulse repetition rate at about 1.007 MHz with increasing pump power in the mode-locked observed range of 219 to 248 mW. In order to examine the stability of the laser, the radio frequency (RF) spectrum is also obtained using a RF spectrum analyzer at input pump power of 244 mW. The spectrum is shown in Fig. 4.8, which indicates the fundamental frequency of 1.0 MHz. This frequency matches to the pulse period (peak to peak duration) of the oscilloscope trace. The RF spectrum has a high signal to noise ratio (SNR) up to 61.75 dB, further indicating the stability of the obtained pulses train.

The mode-locking laser pulses maintained 1.0 MHz repetition rate stably under the maximal pump power of 248 mW during 4 h of continuous operation with excellent repeatability and controllability, and it was further confirmed with over 20 h of mode-locking operation in the following week. No optical damage was observed on the Co-ZnO PVA film under the maximum pump power during these extended hours of continuous operation. Further work on reducing the film loss and optimizing the EDFL cavity is important especially for the high-power operation of the laser.

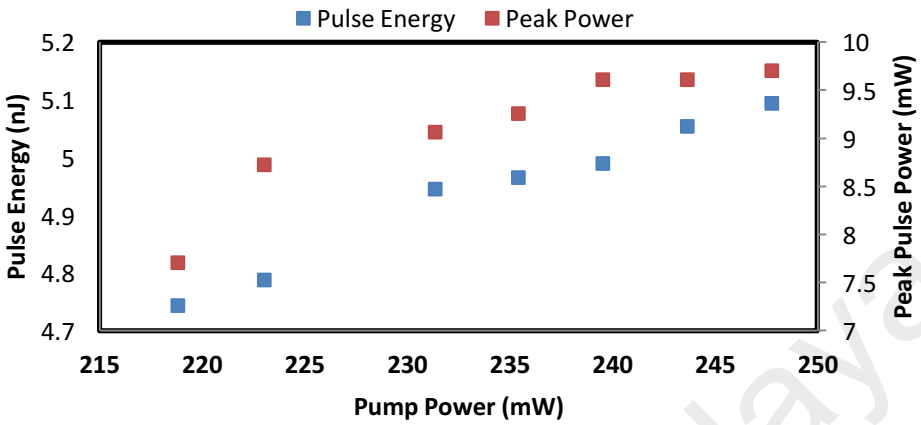

Fig. 4.7: Pulse energy and peak power of the mode-locked laser against the pump Power

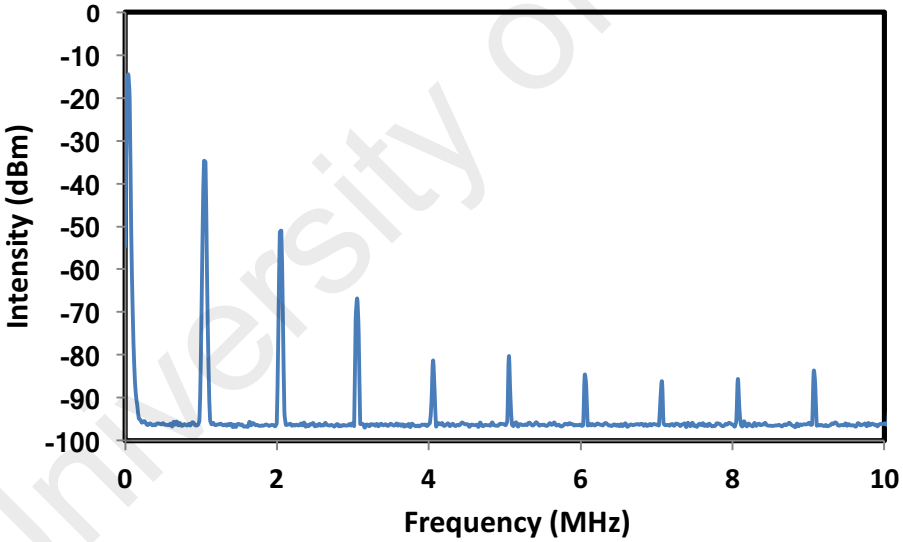

Fig. 4.8: RF spectrum of the mode-locked fiber laser

Chapter 5

Conclusion

The research work aimed to demonstrate pulsed fiber lasers using a cobalt-doped zinc oxide (Co-ZnO) based saturable absorber. At first, the generation of Q-switching pulses train has been successfully proposed and demonstrated using a cobalt-doped zinc oxide (Co-ZnO) nanorods as a SA. The proposed Q-switched Erbium-doped fiber laser (EDFL) operates at 1559.0 nm using the Co-ZnO SA film. The film was fabricated by mixing nanorods Co-ZnO solution with PVA solution and dried it in a room temperature. The film was sandwiched between two fiber ferrules to form the fiber compatible SA device before it is incorporated into a ring EDFL cavity. A stable Q-switched pulse train was obtained as the 980 nm pump power reached the threshold value of 30.5 mW and it continued to operate stably until 109.4 mW. The corresponding pulse repetition rate was tunable from 56.1 to 79.4 kHz. The lowest pulse width was 4.62 μs and the maximum pulse energy was 142 nJ. Our experimental results suggest that Co-ZnO is a promising material for pulsed laser applications.

A passive mode-locked EDFL was then demonstrated based on Co-ZnO nanorods SA using a modified cavity. A long spool of SMF was incorporated into an EDFL to tailor the cavity to operate in anomalous fiber dispersion of -4.571 ps^2 regime. A stable self-started soliton pulses train was generated at threshold pump power of 219 mW. The central wavelength and repetition rate of the laser were 1559.5 nm and 1.007 MHz, respectively. The pulse width and maximum pulse energy obtained are 462.8 ns and 5.1 nJ, respectively at a pump power of 248 mW. The Co-ZnO nanorods film was fabricated by a simple processing technique, and it has a modulation depth of 6 % and saturating intensity of 60 MW/cm^2.

Further works should be dedicated to reduce the film loss and optimizing the EDFL cavity. This is important especially for the high-power operation of the laser.

Bibliography

T, M., & T.Miyashita. (1979). *ultimate low-loss single-mode fiber at 1.55 micro m.* tokyo: electronics letters.

Wolf, E. (1964). *progress in optics* (Vol. 3). N.Y: north-holland publishing co.

koester, C. a. (1964). amplification in a fiber laser. *amplification in a fiber laser*.

Burrus, J. &. (1973). Ebrium-doped fiber amplifier. In P. becker, *Ebrium-doped fiber amplifier* (p. 388). sa diego.

R.J. Mears, L. R. (1985). Neodymium-doped silica single-mode fibre lasers. *electron . lett* , 738-740.

P.Agarwal, G. (2003). *Fiber-optic Communication.* NY: A JOHN WILEY & SONS INC.

SALED, B. E., & TEICH, M. C. (1991). *FUNDAMENTALS OF PHOTONICS.* NY: JOHN WILEY & SONS, INC.

Francis Idachaba, D. U. (2014). Future trends in fiber optics communication. *proceeding of the world congree on engineering 2004 vol 1*, 2-4.

clectrical4u. (n.d.). *electrical4u.com/electrical/wp-content/uploads/2013/05/Components-of-laser.gif*. Retrieved from electrical4u: https://electrical4u.com/electrical/wp-content/uploads/2013/05/Components-of-laser.gif

Frungel, F. B. (2014). *optical pulces - lasers-measuring techniques.* NY: AP.

Frungel, F. B. (2014). *optical pulces-laser-measuring.* Ny: academic press inc.

Mcclung, F., & Hellwarth, R. (1962). Giant optical pulsations from ruby. *applied physics*.

manna, N., & Saha, A. (2011). *Optoelectronics and Optical Communication.* west bengal, india: AN imprint of laxmi publications pvt.ltd.

Ion, J. C. (2005). *Laser Processing of engineering materials.* Elsevier Butterworth-Heinemann.

jia Xu, s. W.-h. (2012, 2014). Nanisecond-pulsed ebrium-doped fiber lasers with graphine saturable absorber. *optics communication*, 4466-4469.

Junsu Lee, J. K. (2014). a femtosecond pulse erbium fiber laser incoporating a saturable absorber based on bulk-structured Bi2Te3 Topological insulator. *optical express*, 6165-6173.

woodward, R. I., & Kelleher, E. J. (2015). 2D Saturable Absorber For Fibre lasers. *applied science*, 1440-1456.

D.I.H Mass, B., & A-R bellancourt, D. S. (2008). High precision optical characterization of semiconductor saturable absorber mirrors. *optical express*, 7571-7579.

Jonah Maxwell Miller. (2011). *Optimizing and Applying Graphene as a saturable absorber.* colorado: University of Colorado Boulder.

Mikael Malmström, O. T. (2016). All-Fiber Nanosecond Gating For Time-Resolved Spectral Analysis. *IEE PHOTONICS TECHNOLOGY LETTERS, 28*, 829-831.

K. TAMURA, E. I. (1993). 77-fs pulse generation from a streched-pulse mode-locked all-fiber ring laser. *optic letters*, 1080-1082.

America, A. M. (2016). *http://www.amadamiyachi.com.* Retrieved from http://www.amadamiyachi.com/servlet/rtaImage?eid=a0g80000002hN4V&feoid=00N80000005Lg3T&refid=0EM80000000RaHi: http://www.amadamiyachi.com/servlet/rtaImage?eid=a0g80000002hN4V&feoid=00N80000005Lg3T&refid=0EM80000000RaHi

R. Paschotta, J. A. (1997, july). Ytterbium-doped fiber amplifiers. *Quantum electrons, 33*(7), 1049-1056.

I.Hartl, M. F. (2013). Ultrafast fiber lasers. *nature research, 7*, 868-874.

Nishizawa, N. (2014). ultrafast pulse fiber laser and their applications. *Applied physics* , 90-101.

R. Holzawarth, T. U. (2000). optical frequency synthesis for precision spectroscopy. *physical review letters, 85*, 2264.

J.-H Lin, C.-C. H.-F. (2007). supercontinum generation in a microstructured optical fiber by picosecond self Q-switched mode-locked Nd:GDVO4 laser. *laser Physics letters, 4*, 413-417.

J. Liu, J. X. (2012). high repetition-rate narrow bandwidth SESAM mode-locked Yb-Doped fiber lasers. *IEEE Photonics Technology Letters, 24*, 539-541.

Keller, U., & Chiu, T. H. (1992). Resonant Passive Mode-locked Nd:YLF Laser. *IEEE journal of Quantum Electronics*, 1710-1718.

M. A. Ismail, S. W. (2012). Nanosecod solition pulse generation by mode-locked erbium-doped fiber laser using single-walled carbon-nanotube-based absorber. *Applied Optics, 51*(36), 8621-8624.

Z. Sun, T. H. (2010). Graphene mode-locked ultrafast laser. *ACS Nano, 4*(2), 803-810.

J. Sotor, G. S. (2014). mode-locking in erbium fiber laser based on mechanically exfoliated Sb2Te3 saturable absorber. *Opt. mater, 4*(1), 1-6.

E. Ismail, N. K. (2016). Black phosphorus crystal as a saturable absorber for both a Q-Switched and mode-locked erbium-doped fiber laser. *RSC Adv., 6*, 72692-72697.

L. Li, Z. W. (2016). Ws2/flourine mica (FM) saturable absorber for high power optical pulse formation. *Optik-int. J. Light Electorn Opt, 127*, 10223-10227.

M. H. M. Ahmed, A. A. (2016). Mode-locking pulse generation with MoS2-PVA saturable absorber in both anomalous and ultra-long normal dispersion regimes. *Applied optics, 55*(15), 4247-4252.

S. G Kumar, a. K. (2017). comparison of modification strategies towards echanced charge carries separation and phocatalytic degradation activity of metal oxide semiconductors (TiO2, WO3 and ZnO). *Applied surface science, 391*, 124-148.

O. A. Yildrium, H. A. (2016). Facile synthesis of cobalt-doped zinc oxide thin films for highly efficient visible light photocatalysts. *Applied Surface Science, 390*, 111-121.

S. C, D. J. (2016). present perspective of broadband photodetectors based on nanobelts, nanoribbons, nanosheets and the emerging 2D materials. *Nanoscale, 12*, 6410-6434.

Wang, Z. L. (2004). Zinc Oxide Nanostructre: growth, properties and application. *condensed Matter, 16*.

Yakuphanoglu, F. (2010, April). Electrical and photovoltaic properties od cobalt doped zinc oxide nanofiber/n-silicon diode. *Alloys and Compounds, 494*(1-2), 451-455.

A. S. Risbud, N. A. (2003). Magnetism in polycrystalline cobalt-substited zinc oxide. *Phys. Rev. B , 68*(20), 205202.

M. H. Huang, Y. H. (2001). Catalytic growth of zinc oxide nanowires by vapor transport. *Advanced Materials, 13*, 113-116.

Funda Aksoy Akgul, G. A. (2016). All solution-based fabrication of copper oxide thin film/cobalt-doped zinc nanowire heterojunctions. *America ceramic Society, 99*(7), 2497-2503.

M. Venkatesan, C. F. (2004, 22 october). Anistropic Ferromagnetism in substituted zinc Oxide. *Phycs. Rev. Lett*(93), 177206.

R. WisnieWski Jakuda, J. M. (2008). Evidence for the linked biogeochemical cycling of zinc, cobalt, and phosphorous in the western atlantic ocean. *Global biogeochemical cycles, 22*, 886-6236.